D3.3 Visualisation of 3D structure using device developed in D3.1 & D3.2

Quanfeng Wang, Alexander Paulus, Han Na, Matthias Saurer, Thomas Eibert

Grant Agreement Number	101099491
Action Acronym	HOLDEN
Action Title	Ethical Design of Holography with Dense wireless Networks (HOLDEN)
Funding Scheme	HORIZON-EIC-2022-PATHFINDEROPEN-01
Version date of the Annex I against which the assessment will be made	13/12/2022
Start date of the project	1/6/2023
Due date of the deliverable	30/11/2024
Actual date of submission	29/11/2024
Responsible	TUM
Contributors	TUM
Dissemination level	Public

European Innovation Council

Funded by the European Union

Funded by the European Union. Views and opinions expressed are, however, those of the author(s) only and do not necessarily reflect those of the European Union or European Innovation Council and SMEs Executive Agency (EISMEA). Neither the European Union nor the granting authority can be held responsible for them. Grant Agreement No: 101099491.

Authors in alphabetical order

Full Name	Organisation	E-mail
Quanfeng Wang	TUM	quanfeng.wang@tum.de
Alexander Paulus	TUM	a.paulus@tum.de
Han Na	TUM	han.na@tum.de
Matthias Saurer	TUM	matthias.saurer@tum.de
Thomas Eibert	TUM	eibert@tum.de

Change History

Version	Date	Status	Author (Company)	Description
1.0	12.11.2024	Final	TUM	First final version

Executive Summary

One of the key innovations within the HOLDEN project is holographic imaging of static environments, i.e., where the imaging scene remains constant while the spatially distributed observation data is acquired. In the process of setting up the corresponding methodologies and algorithms, a variety of test data have been produced by simulation and measurement.

Raw and processed data sets related to these activities are available as open access data sets in order to demonstrate the capabilities of the created methodologies and algorithms.

The data sets, its availability, and its processing are described within this deliverable.

The following contents are covered:

- Short introduction of the HOLDEN project and the collaboration partners
- Description of data structures
- Description of ray-tracing simulations
- Description of FEKO simulations
- Measurements in office environment
- Measurements in anechoic chamber

Table of Contents

Abbreviations

Abbreviation	Description
3D	three-dimensional
Aalto	Aalto University
BPA	back-projection algorithm
CNR	Consiglio Nazionale Ricerche
D3.1	Deliverable 3.1
D3.2	Deliverable 3.2
EC	European Commission
EM	electromagnetic
ESM	Ethics Status Monitor
EU	European Union
HOLDEN	ethical design of holography in dense wireless networks
MoM	method of moments
PEC	perfectly electrically conducting
RF	radio frequency
TOI	target of interest
TUM	Technical University of Munich
TWE	University of Twente
UAV	uninhabited aerial vehicle
VNA	vector network analyser
WP	work package

1. Introduction

1.1. About HOLDEN

The ubiquitous perception by sensing of objects, subjects and gestures is a pivotal challenge for future technology: it enables personalized services such as smart living, automated logistics or interaction through free-space gestures. However, it also challenges ethical and moral boundaries and threatens privacy. HOLDEN proposes a radically new approach to perception by concisely analysing ethical constraints and privacy risks while re-thinking RF-based sensing. We establish necessary conditions for privacy preserving and ethically compliant sensing and develop new paradigms respecting these constraints.

For the first time ever, HOLDEN constitutes a concentrated effort to explore social aspects of RF-sensing to guide the technological advance and to derive technology for ethically and privacy compliant perception. Central to HOLDEN is the development of ethical and privacy constraints. We use these findings to derive privacy and ethically compliant concepts for RF-based perception. We will develop a system of distributed multi-antenna devices for simultaneous multitarget recognition and ubiquitous perception with unprecedented accuracy, which constitutes a radical paradigm shift from a technology-centric perspective to a privacy-centric one via privacy by design.

HOLDEN achieves this goal along three high risk, complementary, and privacy-centric paths:

Path 1: Continuous-space measurement points: Radio-based 3D vision by holographic image processing of RF wavefronts.

Path 2: Discrete-space measurement points: Advanced 3D beamforming for human-scale recognition and tracking through dense massive connected antenna arrays.

Path 3: Signal processing and learning: High-dimensional tensor processing for the distinction of complex activities and motion from massive-dimensional RF data. The resulting breakthrough approaches and algorithms will be compared against application-level benchmarks via usage scenarios in the fields of logistics, smart living, and free-space

1.2. Partners

The consortium consists of four academic partners and a high-tech SME partner: (a) Aalto University (AALTO), Finland, (b) Technical University of Munich (TUM), Germany, (c) Consiglio Nazionale Ricerche (CNR), Italy, (d) University of Twente (TWE), Netherlands, and (e) Adant (Adant), Italy. This consortium features the specialized and complementary expertise required to achieve the project objectives. AALTO will be responsible for the project management (WP1), covered by an experienced and dedicated project manager. Ethical aspects (WP2), will be addressed by TWE (Prof. Ciano Aydin) who is a pioneer in the field. In particular, eventual gender differences in the ethical perception will be taken into account. TUM pioneered RF holography, which makes TUM (Prof. Thomas Eibert) the ideal leader of WP3. In advanced distributed signal and information processing, CNR has through Prof. Stefano Savazzi and Vittorio Rampa more than 14 years of

experience. CNR will lead WP4. Since more than 10 years, AALTO is active in radio sensing and machine learning based activity recognition. This expertise makes AALTO (Prof. Sigg) the ideal leader of WP5. Adant (Daniele Piazza) will contribute to the market analysis, application possibilities, and validation (WP6). Led by AALTO, dissemination with the website as one the media will be addressed by all partners. All academic partners are committed to early publication of results, e.g., via arXiv (open science).

2. Data Structure

The open-source database contains the following type of files:

- ***[Filename*].efe***: ASCII file containing simulated near-field data from the full wave simulation tool FEKO [1], where the key parameters such as frequencies, measured positions, real and imaginary components of the electric fields are included.

- ***aimg_[Filename*].mat***: MATLAB [2] imaging data generated by the algorithms introduced in D3.2, where in particular
  - ***aimg.X*** : x-positions of the imaging domain
  - ***aimg.Y*** : y-positions of the imaging domain
  - ***aimg.Z*** : z-positions of the imaging domain
  - ***aimg.fieldnames*** : names of the included different Cartesian vector components of the imaged sources, e.g., *aimg.fieldnames* = {'x', 'y', 'z'}
  - ***aimg.x*** : x-polarization of the polarimetric imaging results
  - ***aimg.y*** : y-polarization of the polarimetric imaging results
  - ***aimg.z*** : z -polarization of the polarimetric imaging results

- ***[Filename*].nsiascii*** : Containing near-field measurement data, typically S_{12} or S_{21} in dual-polarization from a vector network analyzer (VNA). The frequency information is embedded in the filename, e.g., *6000000000.nsiascii* indicates a frequency of $6\,\mathrm{GHz}$. Other parameters, such as probe positions, VNA setups, as well as the amplitude and phase of the measured signals, are also included in this file.

- ***[Filename*].obj***: Wavefront .obj file, 3D model used for ray tracing simulation.

- ***[Filename*]_EM.mat***: Containing ray-tracing results, specifying the received electric fields at each receiver induced by transmitters at each frequency. It contains the following arrays:
  - ***freq*** : simulation frequencies
  - ***results*** : a vector of structures, each containing the attributes {'E', 'freq'}. The length of the vector corresponds to the length of 'freq', and each 'E' is a 3-dimensional array of size (num_of_Tx, num_of_Rx, 3). This array stores the x-, y-, and z-components of the electric fields at each receiver induced by transmitters.
  - ***tx*** : x-, y- and z-coordinates of each transmitter with a size of (3, num_of_Tx)
  - ***rx*** : x-, y- and z-coordinates of each receive with a size of (3, num_of_Rx)

- ***mannequin_[Filename*]*.mat:** Continuous wave measurement data from a planar scanner. The data is stored in MATLAB [2] data format. The transmission and reflection coefficients between a fixed transmit antenna and a moving (on the planar scanner) antenna, both vertically polarized, are measured for a variety of arrangements of mannequins within a typical office environment.

- **freqs [21x1]**: frequencies of measurements
- **S11 [162x80x21]**: complex-valued reflection coefficient for each measurement location and frequency
- **S21 [162x80x21]**: complex-valued transmission value for each measurement location and frequency
- **X/Y [162x80]**: x- and y-location of the measurement samples

3. Ray Tracing Based Simulations

3.1. Public link

A public link to the dataset is provided as:

Q. Wang, A. Paulus, H. Na, M. M. Saurer, and T. F. Eibert, "RF holography and perception in static environments: Dataset," Oct. 2024. Zenodo. https://doi.org/10.5281/zenodo.13981780

3.2. Description and Visualization

3.2.1. Model of a human person floating in free space

- *Arnold.obj:*

This file contains a 3D model of a male body, named 'Arnold,' represented as a triangular mesh, as shown in Fig. 1, which is utilized for ray tracing simulation as presented in Deliverable 3.1.

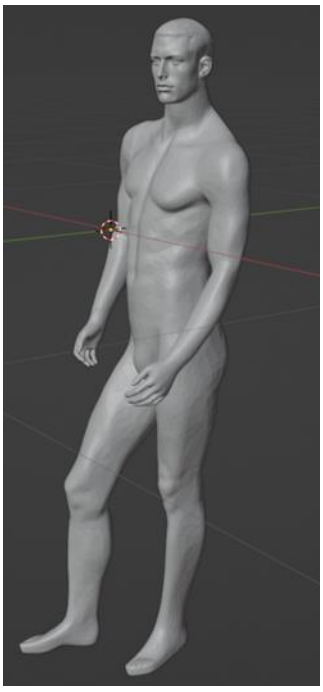

Fig. 1. Display of the 3D model of the male body.

- *Arnold_scene.obj* and *Arnold_scene_with_rays.obj:*

These two files contain the male body model and a corresponding Huygens surface, along with one of the transmitters and part of the receivers (modeled as spheres for illustration), as shown in Fig. 2(a). The file *Arnold_scene_with_rays.obj* includes rays launched by the transmitter and scattered back to the Huygens surface, as illustrated in Fig. 2(b).

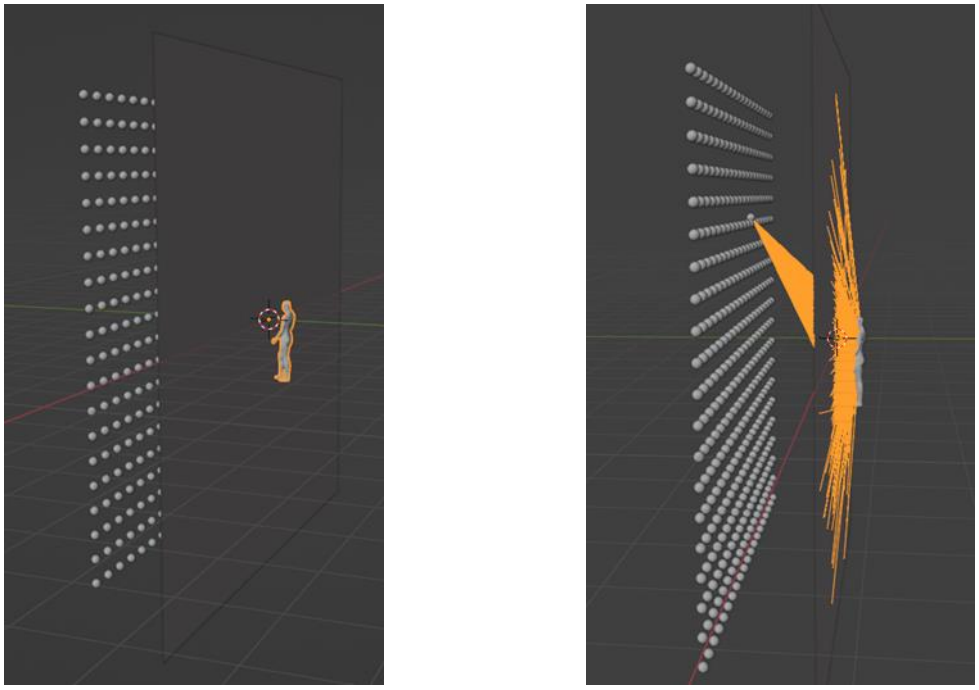

Fig. 2. Ray tracing visualization demo for the male body (illustrating the launch from a single transmitter), (a) with rays, (b) without rays.

- *Arnold_EM.mat:*

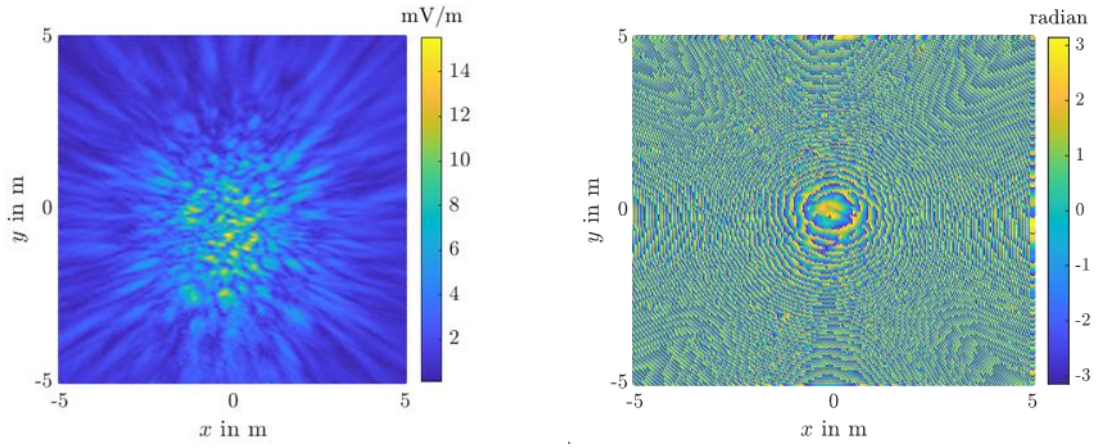

Fig. 3. y-polarization of the received electric field simulated by the ray tracing framework at a frequency of 3.6 GHz, (a) magnitude, (b) phase.

This MAT-file contains synthetic electric field data obtained by ray tracing simulations for all combination of receivers and transmitters for the male body. The simulated data is subsequently used in an imaging routine to reconstruct a three-dimensional holographic image of the human body. A visualization of the magnitude and phase distribution of the electric fields at all receivers, induced by transmitter 50 at a frequency of 3.6 GHz, is shown in Fig. 3.

- *aimg_Arnold.mat:*

This file contains the imaging result generated by a brute-force back-projection algorithm (BPA) using the electric field data simulated by the ray tracer stored in the file *Arnold_EM.mat*. A visualization is demonstrated in Fig. 9.

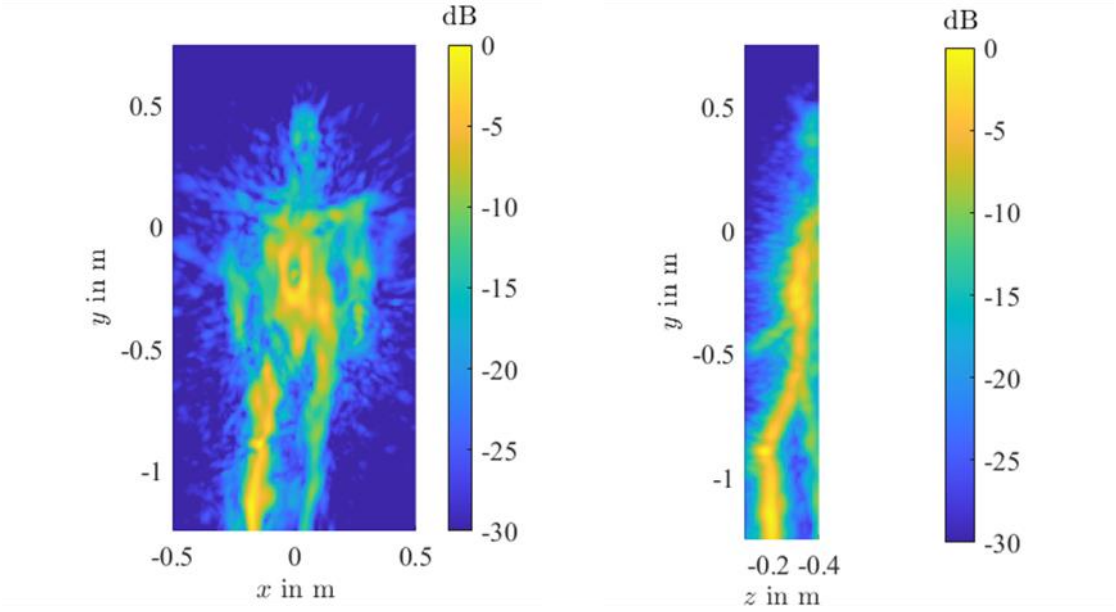

Fig. 4. Imaging results of the male body presented as maximum intensity projections, (a) front view, (b) side view.

3.2.2. Simulation of multi-path propagation employing a PEC ground plane

- *Arnold_Ground_without_Huygens.obj:*

This file contains the model used in the second ray-tracing simulation, which includes the "Arnold" model, the PEC ground plane located at y = 0 m, and the planar transmit and receive array indicated again by small spheres. A schematic visualization of this configuration is given in Fig. 5.

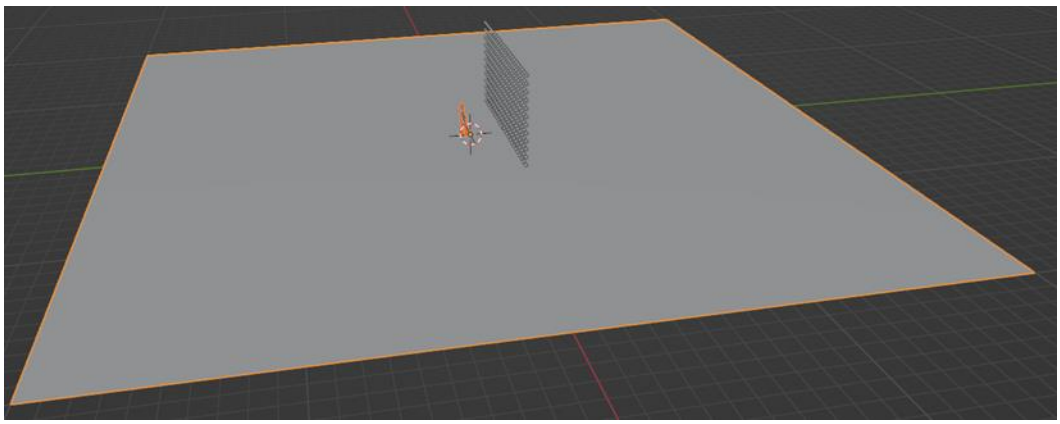

Fig. 5. Display of the 3D model of the male body over a large PEC ground plane.

- *Arnold_Ground_primary_ray_paths.obj,*
  Arnold_Ground_secondary_launch_1_paths.obj

The first file contains rays launched from a specific transmitter toward the human body model, which either strike the scattering object directly or indirectly via reflection off the PEC ground plane, and are tracked until they reach the planar Huygens surface from inside. The second file includes all secondary rays launched from the equivalent surface currents on the Huygens surface, directed toward all receiving positions. This procedure is also visualized in Fig. 6.

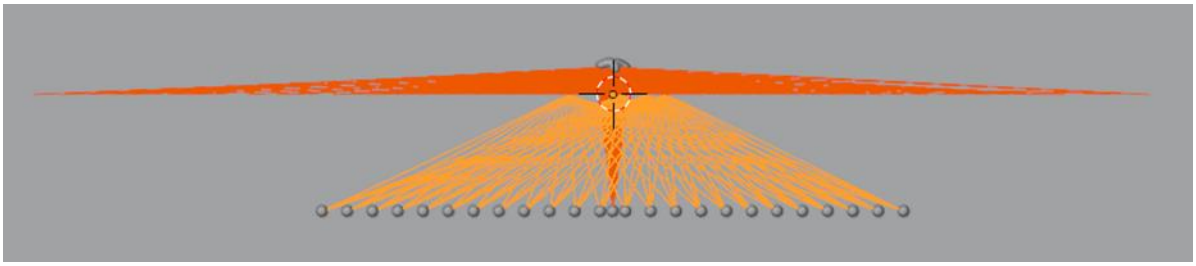

Fig. 6. Ray-path propagation for the Arnold model over a large PEC ground plane.

- *aimg_Arnold_ground.mat:*

This file contains the imaging result generated using the standard BPA with electric field data simulated by the ray tracer, stored in the file *Arnold_mirror_EM.mat*. The image principle is applied to enhance the imaging process, made possible by the presence of the PEC ground plane. The image generation involves coherently superimposing four possible combinations of the transmit and receive arrays with the corresponding mirrored transmit and mirrored receive arrays. A graphical visualization is demonstrated in Fig. 7.

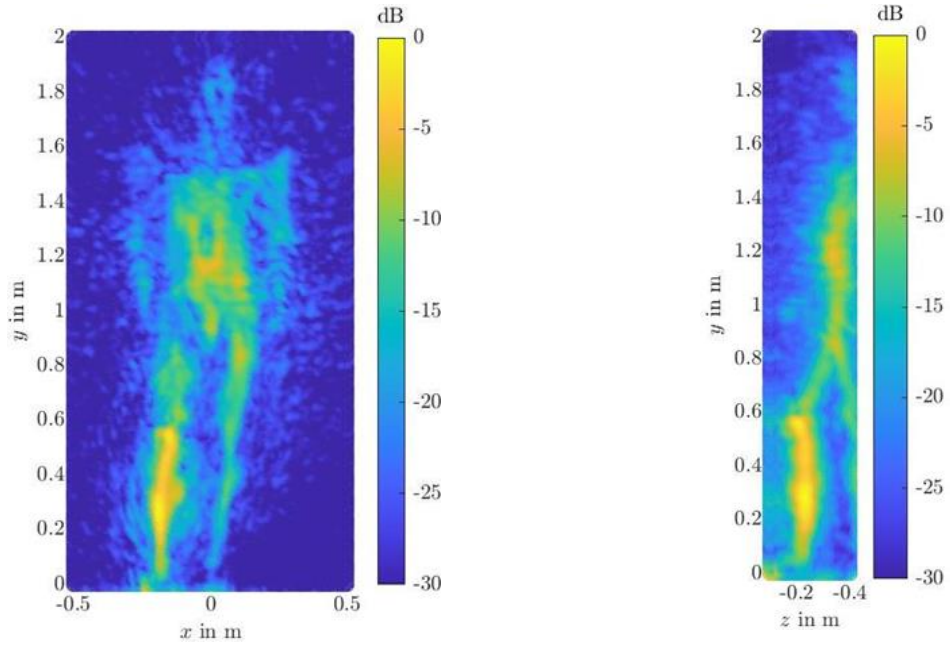

Fig. 7. Imaging results of the male body over ground using the BPA and the image principle presented as maximum intensity projections, (a) front view, (b) side view.

4. FEKO Simulations

4.1. Public Link

A public link to the dataset is provided as:

Q. Wang, A. Paulus, H. Na, M. M. Saurer, and T. F. Eibert, "RF holography and perception in static environments: Dataset," Oct. 2024. Zenodo. https://doi.org/10.5281/zenodo.13981780

4.2. Description and Visualization

- *Dipole_Sphere3.efe*:

This ASCII file contains simulation data from FEKO based on the method of moments (MoM). The simulated scenario is shown in Fig. 8, where a y-polarized Hertzian dipole, represented by a yellow arrow, is positioned at (-0.5 m, 0 m, 0.5 m). The three perfectly electrically conducting (PEC) spherical scatterers are centered at (0 m, 0 m, 0 m), (0.3 m, 0 m, 0 m) and (0.6 m, 0 m, 0 m), respectively. The radius of each scattering sphere is 0.01 m. The tangential components of both the incident electric field from the illuminating dipole and the field scattered from the spheres are collected over a closed spherical surface with a radius of 1.0 m. The radiation frequency spans from 8 GHz to 10 GHz with a step frequency of 0.2 GHz.

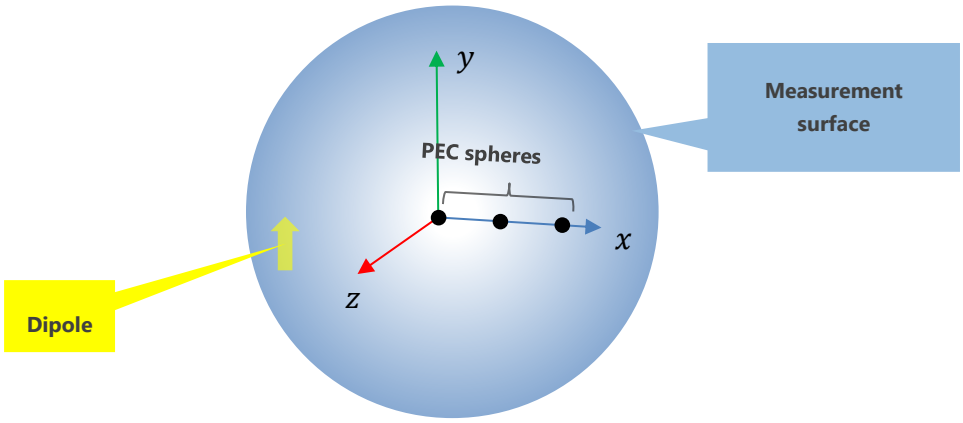

Fig. 8. Illustration of the simulation setup including three spheres as scatterers and a Hertzian dipole serving as the illumination source. The tangential electric field is collected over a spherical surface.

Utilizing the imaging algorithm and phase correction method introduced in D3.2, the corresponding imaging result is obtained and stored in the MATLAB file *aimg_simu_spheres.mat*. This file contains the coherent superposition of the three polarimetric components across all frequencies and can be used for various visualizations of the target of interest (TOI). For instance, the imaging result combining all three polarimetric components is displayed in Fig. 9.

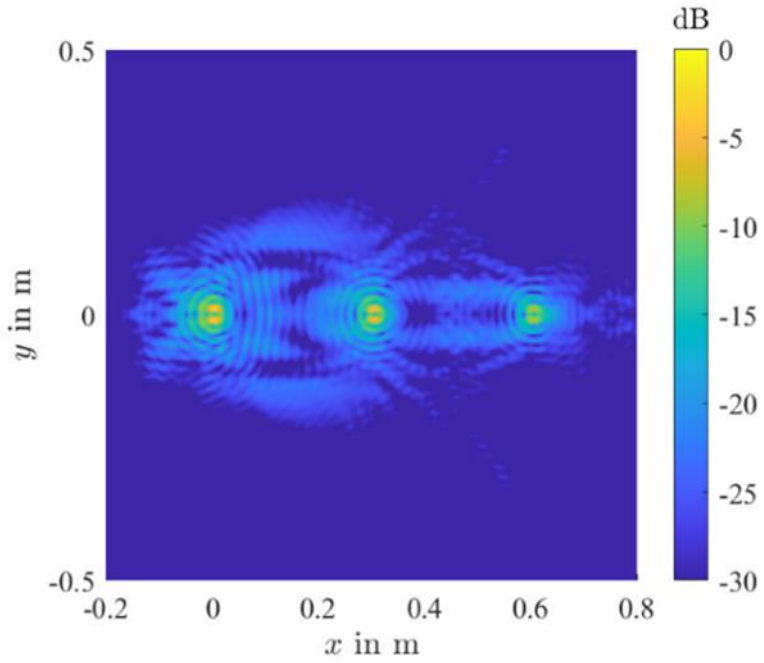

Fig. 9. Imaging result of the three spheres in the plane z = 0 m.

- *Horn_Plate_NearField1.efe:*

The second simulation scenario involves a horn antenna and a rectangular plate with various holes and rectangular cutouts, as illustrated in Fig. 10. The plate is illuminated by the horn antenna at an angle of approximately 45 degrees. The plate is placed at the origin of the coordinate system, while the horn antenna is located at the coordinates x = 0.45 m, y = 0.45 m, z = 0 m. Both the antenna and the plate are made of perfectly electrically conducting (PEC) material. The length, width and thickness of the plate is 0.2 m, 0.2 m and 0.01 m, respectively. The x and z components of the electric field were collected over a rectangular aperture in the plane y = 1 m extending from x = −0.7 m, z = -0.5 m to x = 0.7 m, z = 0.5 m each sampled at 10 000 uniformly distributed measurement points.

The frequencies used are linearly distributed from 8 GHz to 10 GHz, with a step size of 50 MHz. The simulated electric fields stored in this file can also be extracted and used for visualization. For instance, the z-component is normalized to its maximum value and shown in Fig. 11(a), while the corresponding phase information is given in Fig. 11(b).

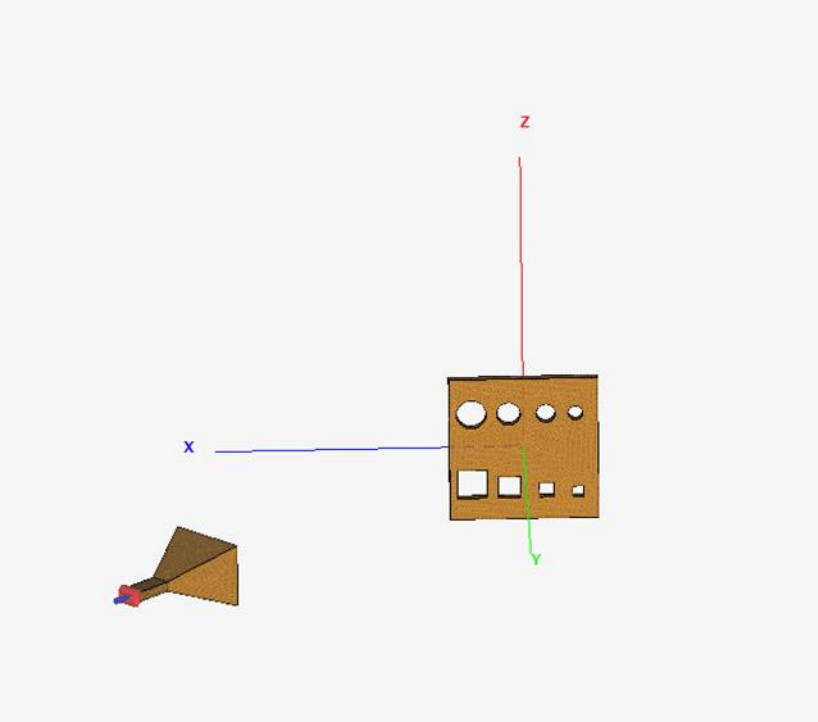

Fig. 10. Illustration of the simulation setup in FEKO including a rectangular plate as the scattering object and a horn antenna serving as the illumination source.

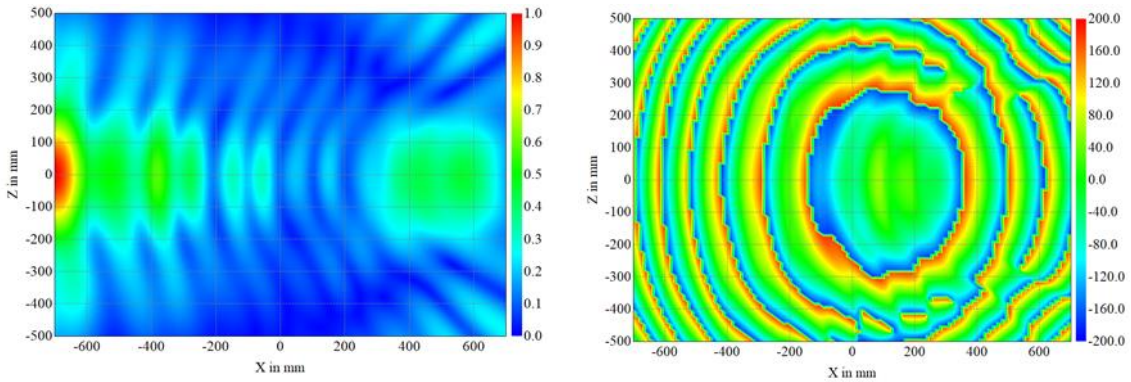

(a) (b)

Fig. 11. The simulated near-fields for the z-component of the electric field at 8 GHz. (a) The normalized magnitude. (b) The phase information in degree.

The image results for the horn antenna and the plate are stored in the MATLAB files *aimg_simu_horn.mat* and *aimg_simu_plate.mat*, respectively. Both files contain 3D volumetric imaging data, allowing for various visualization techniques. For example, 2D imaging results at specific cut planes are shown in Fig. 12(a) and Fig. 12(b). In this instance, the horn antenna is displayed at the cut plane y = 0.45 m, and the front side of the plate is shown at the plane y = 0.01 m.

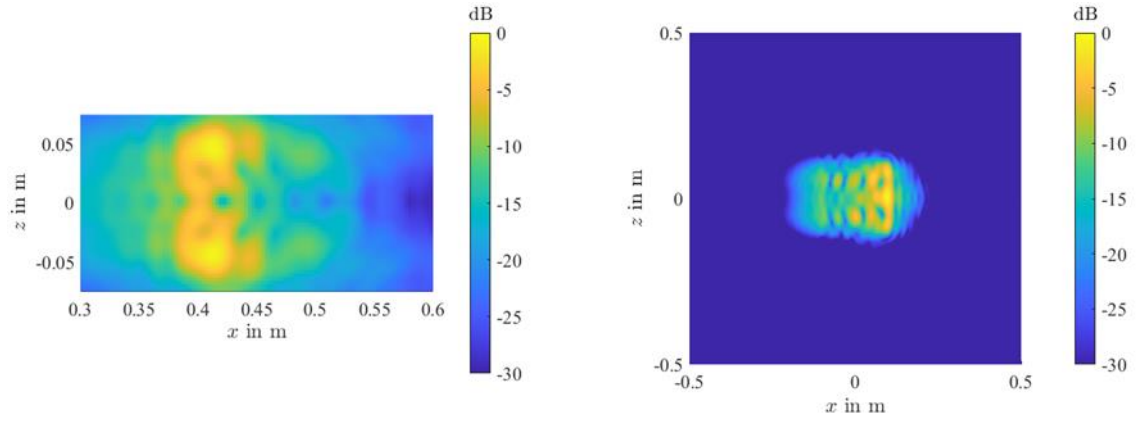

(a) (b)

Fig. 12. Imaging results for the horn antenna and the metallic plate in (a) and (b), respectively.

5. Measurements – Planar Office Scanner

5.1. Public Link

A public link to the dataset is provided as:

Q. Wang, A. Paulus, H. Na, M. M. Saurer, and T. F. Eibert, "RF holography and perception in static environments: Dataset," Oct. 2024. Zenodo. https://doi.org/10.5281/zenodo.13981780

5.2. Description and Visualization

A two-axis planar scanning system has been installed on a side wall of a typical office room at the Chair of High-Frequency Engineering, Department of Electrical Engineering, School of Computation, Information and Technology of the Technical University of Munich. The setup, of which a photograph is shown in Fig. 13, allows the acquisition of the radio transmission (S_{21} parameter acquired with a VNA) between a fixed transmit antenna (vertically/y-polarized) and a moving probe antenna (vertically/y-polarized), which is moved by the scanner system on a surface of approximately 4.98 m x 2.46 m (excluding margins for safety). The transmission between both antennas is recorded within the frequency range from 2.4 GHz to 2.5 GHz, where the surface of the wall is sampled with a resolution of approximately 3 cm, resulting in 162 x 80 = 12960 samples for a full measurement. All measurements have been performed in a step-mode manner, where a S_{21} sample is recorded after moving the probe to a desired x- and y-position and waiting for vibrations of the platform to decay. A full measurement takes around 17 hours and 3 full measurements are provided. A NanoVNA600A [3] was used for all measurements, where additional amplifiers and filters have been added in the signal path. The raw data of a typical measurement is shown in Fig. 14, where the wave-like behavior in the phase data already indicates the presence of a dominant radiation source.

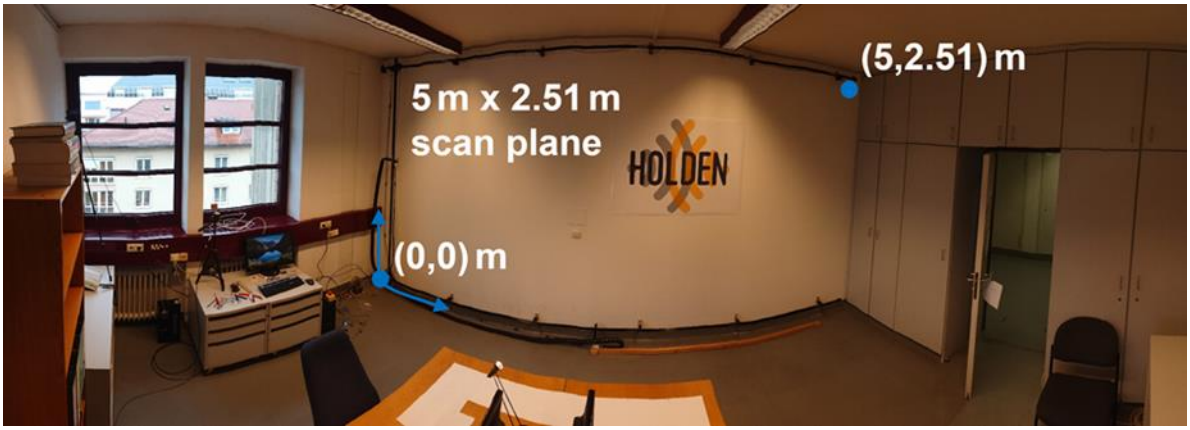

Fig. 13. Wide-angle photograph of the planar scanner installed in an office at TUM.

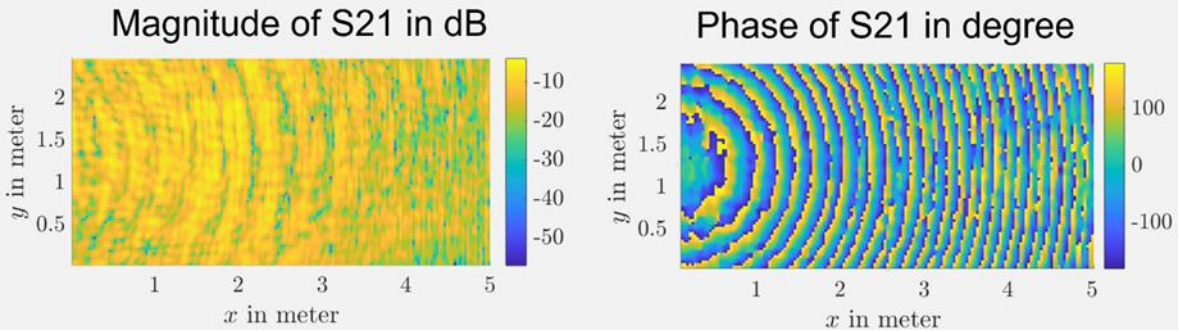

Fig. 14. Typical measured transmission data within the office environment. Illustration of the magnitude of the transmission (left) in dB and the corresponding phase information (right) in degree.

The three different measurements belong to three different arrangements of plastic/wooden mannequins (shown in Fig. 15), where either none one or two mannequins are present within the office, as illustrated in Fig. 16 (a), (b) and (c), respectively. In order to reassemble the interaction between electromagnetic waves in the low-GHz frequency range with real human bodies as closely as possible, the mannequins where painted with zinc-aluminium spray before being employed in the measurement campaign (not shown here). This zinc-aluminium paint was found to be a suitable and cheap alternative to silver- or copper-based conductive paints.

Further details, images and explanations of the measurement setup and hardware are provided in the "TUM_HFT_WiFi_Mannequins_Documentation_Public_12_09_2024.pptx" file, which is available in the public repository.

Fig. 15. Female and male mannequins used for the measurements.

The measurement data is provided in the form of MATLAB [2] files, which contain the following variables:

- **freqs [21x1]**: frequencies of measurements
- **S11 [162x80x21]**: complex-valued reflection coefficient for each measurement location and frequency (made available mostly for the reason of completeness, usability limited)
- **S21 [162x80x21]**: complex-valued transmission value for each measurement location and frequency
- **X/Y [162x80]**: x- and y-location of the measurement samples

In order to further illustrate the measurement setup, one video consisting of sequences of snapshots acquired from a webcam and surveilling the measurement arrangement are provided in the files "Exemplary_measurement.mp4", which showcases the process of a single measurement, in the form of a time lapse, and consists of snapshots taken at every 100th measurement location.

(a) (b) (c)

Fig. 16. Three different arrangements of the mannequins within the room with basic equipment. (a) Without mannequins. (b) With only female mannequin. (c) With both female and male mannequins.

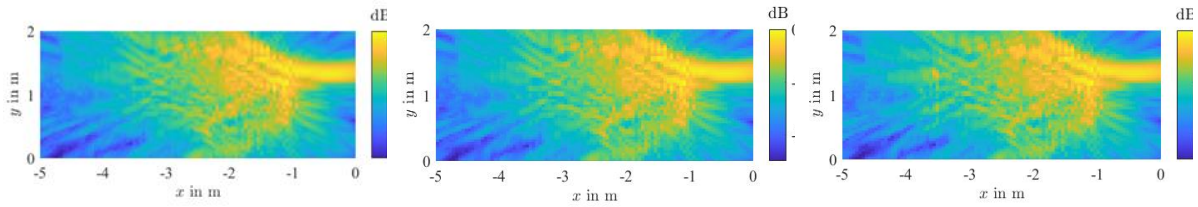

(a) (b) (c)

Fig. 17. Imaging results of the three different arrangements of the mannequins within the room with basic equipment. (a) Without mannequins. (b) With only female mannequin. (c) With both female and male mannequins.

Similarly, by applying the methodology presented in Deliverable 3.2, imaging results for these three arrangements are obtained. Visualizations of the maximum intensity projection in the xy-plane are shown in Fig. 17 (a), (b) and (c), respectively. However, due to the complex indoor environment and limited bandwidth, all results are nearly identical and none of them shows a good alignment with the measurement. Therefore, using the measurement without mannequins

as the background, the imaging results corresponding to Fig. 17(b) and (c) after background subtraction are shown in Fig. 18(a) and (b), where outlines of the mannequins and part of the desk are recognizable.

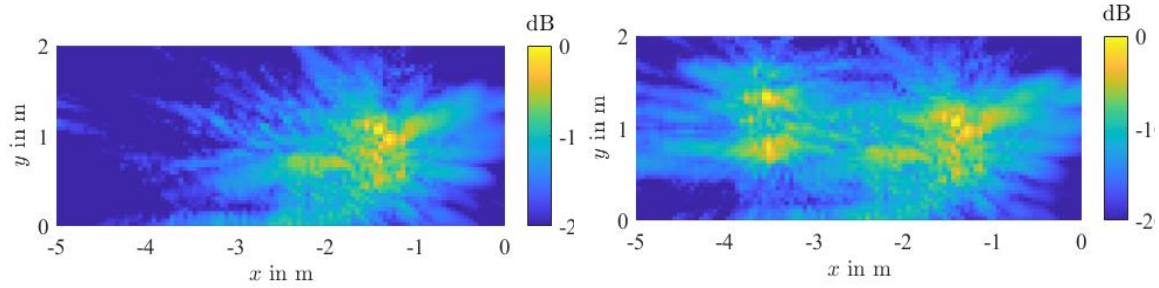

(a) (b)

Fig. 18. Imaging results after background subtraction. (a). Only female mannequin is placed in the room. (b) Both female and male mannequins are placed in the room.

6. Measurements – Anechoic Chamber

6.1. Public Link

A public link to the dataset is provided as:

Q. Wang, A. Paulus, H. Na, M. M. Saurer, and T. F. Eibert, "RF holography and perception in static environments: Dataset," Oct. 2024. Zenodo. https://doi.org/10.5281/zenodo.13981780

Part of the data and results are found in [4] and [5].

6.2. Description and Visualization

A measurement campaign was conducted in the anechoic antenna measurement chamber at the Chair of High- Frequency Engineering, Technical University of Munich. The measurement setup is depicted in Fig. 19. An uninhabited aerial vehicle (UAV) carrying three quad-ridge Vivaldi antennas is fixed to the rotation stage of the spherical positioner close to the origin of the measurement coordinate system. Two double-ridged horn antennas are utilized as the illuminating antenna and the scanning probe. The probe was mounted on a planar scanner capable of moving along the x- and y- direction at z = 2.8 m. Data for both co-polarization and cross-polarization were collected and stored in the provided **.nsiascii* files. The frequency spans, with a step size of 0.05 GHz, cover two different bandwidths, from 1 GHz to 6 GHz and from 6 GHz to 12 GHz, respectively.

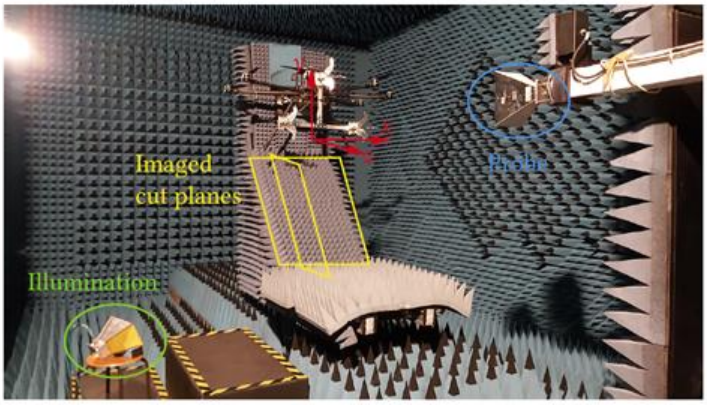

Fig. 19. Measurement configuration utilized in the anechoic chamber. The origin of the coordinate system is set close to the location where the UAV is placed. ©2024, IEEE

In this measurement, the target of interest (TOI) can be chosen as the illuminating horn antenna, the UAV, or even the electromagnetic wave absorbers. The corresponding imaging results obtained by the methodology presented in Deliverable 3.2 are provided in MATLAB files:

- *aimg_source.mat* : Imaging data of the illumining antenna in the volume defined as a cube with dimensions $-1.7\ \text{m} \leqslant x \leqslant -1.2\ \text{m}$, $-1.3\ \text{m} \leqslant y \leqslant -0.8\ \text{m}$, and $1.0\ \text{m} \leqslant z \leqslant 1.5\ \text{m}$.

- *aimg_UAV.mat* : Imaging data of the UAV in the volume defined as a cube with dimensions −0.75 m $\leqslant x \leqslant$ 0.75 m, −0.1 m $\leqslant y \leqslant$ 0.6 m, and 0.0 m $\leqslant z \leqslant$ 1.5 m. Several different visualizations can be achieved based on this file, such as maximum intensity projections and iso-surface as shown in Fig. 20.
- *aimg_absorber_3D.mat* : The imaging data of the wave absorbers in the volume consists of several planes parallel to the slope on which the absorbers are mounted, as illustrated in Fig. 21. Specifically, the region is defined by 0.37 m $\leqslant x \leqslant$ 1.4 m, −0.5 m $\leqslant y \leqslant$ 0.5 m and z = −0.9y+0.2 m. Two different cut planes, one parallel and the other perpendicular to the slope, are provided as examples, as shown in Fig. 19.

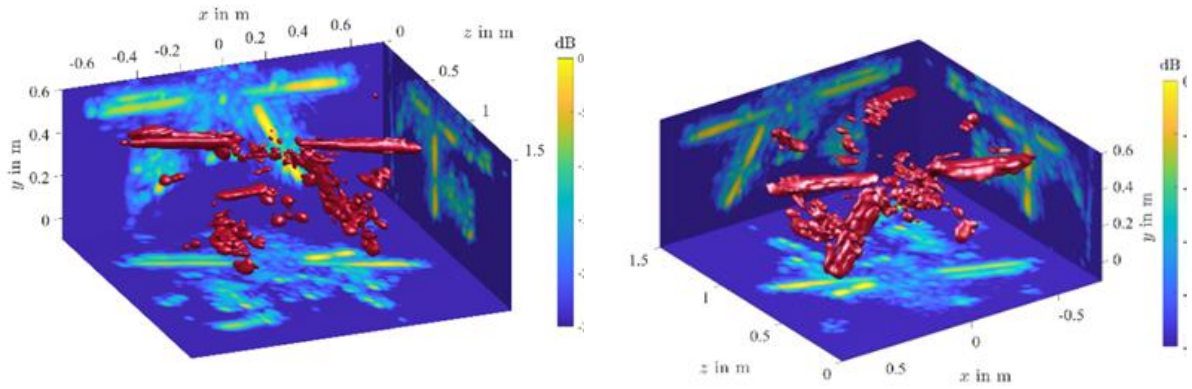

Fig. 20. 3-D visualization of the imaged UAV. (a) Viewed from a perspective oriented towards the negative z-direction. (b) Viewed from a perspective oriented towards the positive z-direction.

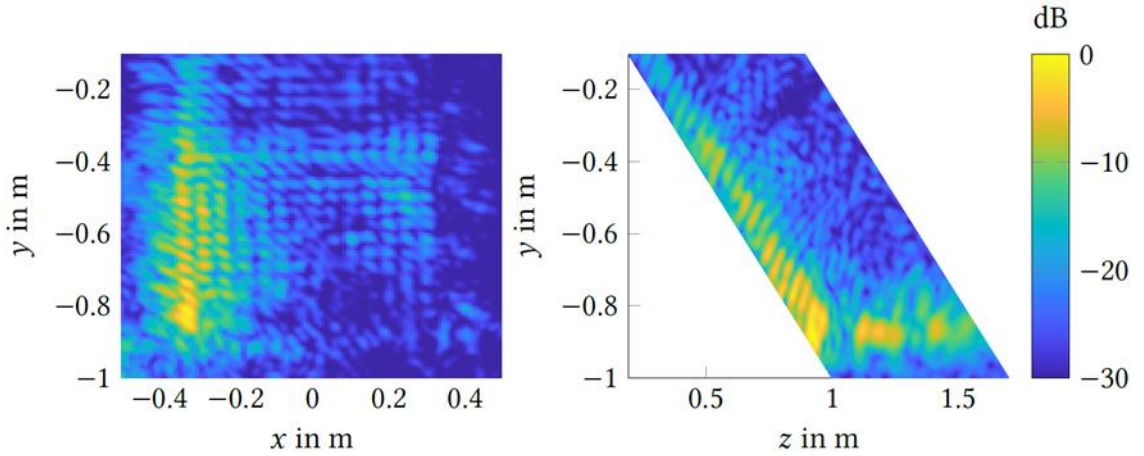

Fig. 21. Imaging results of the absorbers, (a) in plane parallel to the absorbers with $z = -0.9y + 0.2\,\mathrm{m}$, (b) in plane perpendicular to the absorbers with x = −0.33 m. ©2024, IEEE

7. Summary

An efficient simulation framework by virtue of a ray tracing engine, which allows for the simulation of complex indoor scenarios has been presented in D3.1. In addition, based on the concerns (and potential opportunities) that have been collected and expressed by all project partners in the ethics status monitor (ESM) [6], a 3D holographic imaging algorithm based on the concept of passive radar has been thoroughly introduced in D3.2.

In the course of the HOLDEN project research, various simulations and experimental measurement data were utilized to test and support the validation of the proposed algorithm. A wide collection of raw data have been uploaded and made open-source on the corresponding platform. In this deliverable, detailed descriptions of these data are provided, along with the final imaging results generated by the corresponding imaging algorithms, which are made available for visualization.

In this deliverable, public links to all open-source data are included. Detailed descriptions of the raw data from all simulations and measurements, as well as descriptions and visualizations of the holographic 3D data generated by the corresponding imaging algorithms, have been provided.

8. References

[1] Altair. (2023) FEKO. [Online]. Available: https://altairhyperworks.com/product/FEKO.

[2] The MathWorks, Inc. (2023). [Online]. Available: https://www.mathworks.com.

[3] NanoRFE VNA6000-A. [Online]. Available: https://nanorfe.com/vna6000.html.

[4] Q. Wang, M. M. Saurer, and T. F. Eibert, "3D near-field passive radar imaging utilizing phase corrected frequency domain inverse source reconstructions," IEEE Trans. Antennas Propag., submitted, also to TechRxiv.

[5] Q. Wang and T. F. Eibert, "Microwave imaging of electromagnetic wave absorbers in an antenna measurement chamber," in IEEE Int. Symp. Antennas Propag., Jul. 2024, pp. 1139–1140.

[6] S.I. Cammers-Goodwin, N. Gertz, C. Aydin, T. Eibert, M. Nagenborg, S. Savazzi, S. Sigg, "D8.9 ethics status monitor (ESM)", Oct. 2024, Available: https://holden-project.eu/deliverables/

9. Table of Figures